Double-Gated Myocardial ASL Perfusion Imaging Is Robust to Heart Rate Variation

Hung Phi Do,[1]* Andrew J. Yoon,[2] Michael W. Fong,[2] Farhood Saremi,[3] Mark L. Barr,[4] and Krishna S. Nayak[5]

Purpose: Cardiac motion is a dominant source of physiological noise (PN) in myocardial arterial spin labeled (ASL) perfusion imaging. This study investigates the sensitivity to heart rate variation (HRV) of double-gated myocardial ASL compared with the more widely used single-gated method.

Methods: Double-gating and single-gating were performed on 10 healthy volunteers (n = 10, 3F/7M; age, 23–34 years) and eight heart transplant recipients (n = 8, 1F/7M; age, 26–76 years) at rest in the randomized order. Myocardial blood flow (MBF), PN, temporal signal-to-noise ratio (SNR), and HRV were measured.

Results: HRV ranged from 0.2 to 7.8 bpm. Double-gating PN did not depend on HRV, while single-gating PN increased with HRV. Over all subjects, double-gating provided a significant reduction in global PN (from 0.20 ± 0.15 to 0.11 ± 0.03 mL/g/min; $P = 0.01$) and per-segment PN (from 0.33 ± 0.23 to 0.21 ± 0.12 mL/g/min; $P < 0.001$), with significant increases in global temporal SNR (from 11 ± 8 to 18 ± 8; $P = 0.02$) and per-segment temporal SNR (from 7 ± 4 to 11 ± 12; $P < 0.001$) without significant difference in measured MBF.

Conclusion: Single-gated myocardial ASL suffers from reduced temporal SNR, while double-gated myocardial ASL provides consistent temporal SNR independent of HRV. **Magn Reson Med 77:1975–1980, 2017. © 2016 International Society for Magnetic Resonance in Medicine**

Key words: myocardial perfusion imaging; arterial spin labeling; cardiovascular magnetic resonance; physiological noise; myocardial blood flow; heart rate variation

INTRODUCTION

Myocardial perfusion and perfusion reserve are important indicators of coronary artery disease (CAD) status. Single positron emission computed tomography (SPECT) is the most widely used clinical test for assessing myocardial perfusion and perfusion reserve, but has limitations related to the use of ionizing radiation (1,2). In recent years, first-pass perfusion MRI has demonstrated improved sensitivity and specificity (3). The main limitation of first-pass perfusion is the required use of Gadolinium-based contrast agents that can be toxic to patients with renal dysfunction (4,5).

Arterial spin labeled (ASL) MRI is a noncontrast technique that is capable of quantifying tissue perfusion (6). Unlike SPECT and first-pass MRI, ASL uses blood itself as the tracer, and is, therefore, completely safe and repeatable. ASL is widely used in the brain for assessment of neuropathological diseases (7,8) but its application to the heart is still an active area of research (9). Myocardial ASL has been adapted and developed for more than a decade on human and animal models (10–19). Flow-sensitive alternating inversion recovery (FAIR) (20,21) is the most widely used approach and has been implemented in two ways: (i) T_1 apparent approach (10–14) that uses curve fitting and (ii) subtraction approach (15–18) that uses Buxton's general kinetic model (22) for quantification.

Both approaches have been shown to quantify myocardial perfusion and perfusion reserve. The latter is simpler and has been more widely adopted in recent years, but it requires the same post labeling delay (PLD) in paired control and labeled images. This restriction makes it sensitive to heart rate variation (HRV) because either the labeling pulse or image acquisition can be cardiac-triggered in real-time, but not both. The paired images are typically acquired 8–10 s apart, within one breath-hold, to minimize respiratory motion. In cases of significant HRV, the labeling pulses, control images, and labeled images will occur during different cardiac phases and thus experience inconsistent cardiac motion. This has been shown to be a dominant source of physiological noise (PN) (18). HRV may arise from arrhythmias and changes in heart rate due to anxiety, subject motion, deep breathing, or arousals from sleepiness during the examination. HRV can also occur during free breathing (23), breath-holds (24–26), physical stress (27), and pharmaceutical stress with adenosine (28).

Poncelet et al first introduced double-gated myocardial ASL (10), which is believed to be less sensitive to cardiac motion because it allows both labeling and image acquisition to occur in the same cardiac phase (i.e.,

[1]Department of Physics and Astronomy, University of Southern California, Los Angeles, California, USA.
[2]Department of Medicine, Division of Cardiology, Keck School of Medicine of USC, University of Southern California, Los Angeles, California, USA.
[3]Department of Radiology, Keck School of Medicine of USC, University of Southern California, Los Angeles, California, USA.
[4]Department of Cardiothoracic Surgery, Keck School of Medicine of USC, University of Southern California, Los Angeles, California, USA.
[5]Ming Hsieh Department of Electrical Engineering, University of Southern California, Los Angeles, California, USA.

Grant sponsor: L.K. Whittier Foundation; Grant number: 0003457-00001; Grant sponsor: American Heart Association; Grant number: 13GRNT13850012; Grant sponsor: Coulter Foundation Clinical Translational Research Award.

*Correspondence to: Hung Phi Do, MS, 3740 McClintock Avenue, EEB 400, University of Southern California, Los Angeles, CA 90089-2564. E-mail: hungdop@gmail.com

Received 28 December 2015; revised 27 April 2016; accepted 1 May 2016
DOI 10.1002/mrm.26282
Published online 30 May 2016 in Wiley Online Library (wileyonlinelibrary.com).

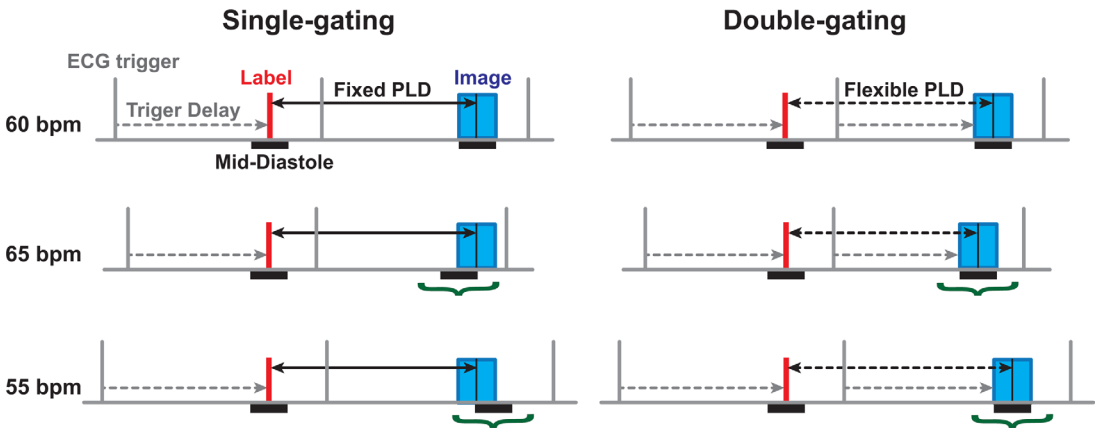

FIG. 1. Sequence diagram of single-gated and double-gated myocardial ASL. In single-gating, only labeling pulse is cardiac-triggered (dashed arrows) and the postlabeling delay (PLD) is kept constant (solid two-sided arrows) for both control and labeled images. As such, the imaging window will deviate from mid-diastole in the presence of HRV (+5 bpm and -5 bpm in the 2nd and 3rd row, respectively). In double-gating, both labeling and imaging are cardiac-trigged (dashed arrows), and the PLD is allowed to be different (dashed two-sided arrows) for control and tagged images. Hence, the timing of image acquisition is adjusted in real-time to be centered around mid-diastole.

termed "double-gating") but, to date, this has not been well-validated experimentally. Poncelet et al successfully demonstrated double-gating in swine and healthy human volunteers, but their technique was prohibitively long with high noise levels even during rest flow measurements.

In this study, we demonstrate that double-gated myocardial ASL is robust to HRV compared with a single-gated approach in healthy human volunteers and heart transplant recipients.

METHODS

Experimental Methods

The study was approved by our Institutional Review Board, and written informed consent was obtained from all participants. Ten healthy adult subjects (n = 10, 3F/7M; age, 23–34 years) and eight heart transplant recipients (n = 8, 1F/7M; age, 26–76 years) participated in the study. All experiments were performed on a 3 Tesla (T) system (Signa Excite HDxt, GE Healthcare) using an eight-channel cardiac array. Myocardial ASL perfusion imaging was performed using FAIR with balanced steady state free precession (SSFP) image acquisition.

In each subject, a mid-ventricular short-axis slice was identified. Double-gated and single-gated myocardial ASL scans were performed in a randomized order. Scan time was approximately 3 min per scan. Each ASL scan comprised of seven breath-holds. The first 5-s breath-hold was comprised of a baseline image (without labeling pulse) and an inversion check (pulsed label applied immediately before image acquisition). The next six 12-s breath-holds were each comprised of one control and one labeled image.

Pulse sequence diagram of single-gating and double-gating are shown in Figure 1. Single-gated myocardial ASL was implemented as previously described (16,18) where the labeling pulse is cardiac-triggered (dashed arrows) and the postlabeling delay (PLD) is kept constant (solid two-sided arrows) for both control and labeled images.

As such, the imaging window will deviate from mid-diastole in the presence of HRV (+5 bpm and −5 bpm in the 2nd and 3rd row, respectively). Double-gated myocardial ASL was implemented in a similar manner as the single-gated method except that both labeling and imaging were cardiac-triggered in real-time. When using double-gating, both labeling and imaging are cardiac-trigged (dashed arrows), and the PLD is allowed to be different (dashed two-sided arrows) for control and tagged images. Hence, the timing of image acquisition is adjusted in real-time to be centered around mid-diastole. In this study, the trigger delay (TD) was set to be 75% of the most recently computed R-R interval (29) for both single-gating and double-gating. In double-gating, precise inversion time was achieved by using an "adaptive recovery time" method (30). The adaptive recovery time method was implemented by playing a series of 2-ms wait-pulses after the inversion pulse until the next R-wave was detected.

Single-gated and double-gated myocardial ASL were performed with identical sequence parameters that are echo time (TE) = 1.4 (1.3–1.5) ms, repetition time (TR) = 3.2 (3.0–3.5) ms, flip angle = 50°, slice thickness = 10 mm, field-of-view = 210 (160–260) mm, matrix size = 96 × 96 with parallel imaging generalized autocalibrating partially parallel acquisitions (31) rate 1.6, and 19-TR Kaiser-Bessel ramp-up and ramp-down pulses. The Kaiser-Bessel ramp-up is the optimal scheme for mitigating transient oscillations in balanced SSFP imaging (32). The Kaiser-Bessel ramp-down optimally preserves longitudinal magnetization after image acquisition. A ramp duration of 19-TRs was chosen to match prior work (18). A fat-saturation pulse was applied immediately before the ramp-up pulses. Nonselective hyperbolic secant adiabatic inversion pulse was used for labeling. A 30 mm slice-selective inversion slab was used for the control image. The heart rate was recorded in all scans for evaluation of HRV.

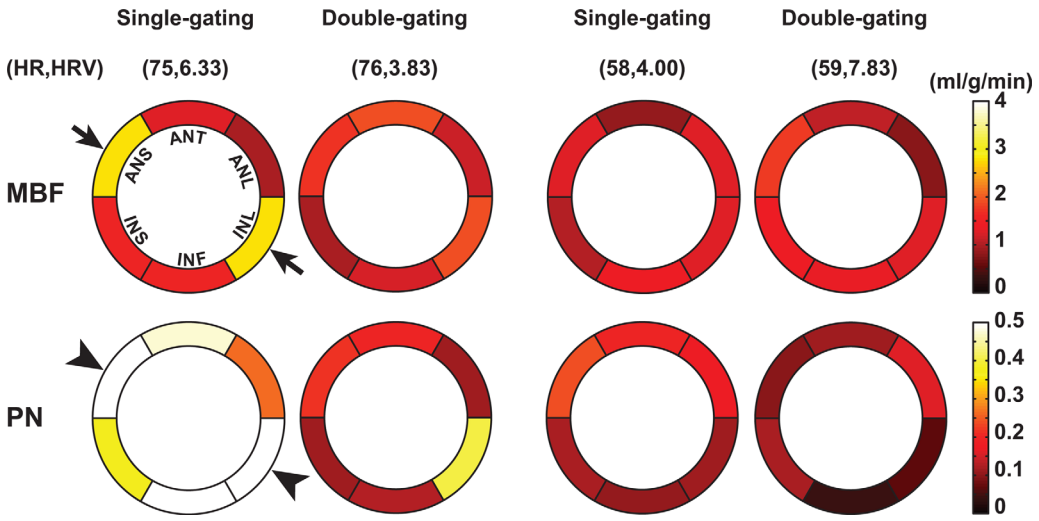

FIG. 2. MBF and PN maps from single-gated and double-gated myocardial ASL in two representative subjects. Lower PN is observed in double-gating compared with single-gating in both subjects. The MBF maps show good agreement between the two methods except in two segments (arrows) that might be explained by higher PN in the single-gating method (arrowheads). ANT, anterior; ANS, anteroseptal; INS, inferoseptal; INF, inferior; INL, inferolateral; ANL, anterolateral.

Data Analysis

Left ventricular myocardium was manually segmented for global and per-segment (six segments) analysis. The entire left ventricular myocardium region of interest (ROI) was used for global analysis, while the AHA six-segment model (33) of a short axis slice was used for per-segment analysis. Single-gated myocardial blood flow (MBF) was calculated using Buxton's general kinetic model (22) as previously described (16,18). Double-gated MBF was quantified using the same equation but with interpolated signal difference from control and tagged T_1 curves as previously described (10). PN is a measure of the variability of measured MBF and is measured in mL/g/min. PN is defined as the standard deviation of six repeated MBF measurements as described in Zun et al (16). Both single-gated and double-gated PN were calculated identically. Temporal SNR (MBF/PN) was also calculated from the two methods.

HRV was defined as the average absolute difference between the instantaneous heart rate when control and labeled images were acquired. The data were then divided into two subgroups: low HRV ($n = 9$; HRV < 4 bpm) and high HRV ($n = 9$; HRV ≥ 4 bpm). MBF, PN, and temporal SNR measured from the two methods were compared in the two subgroups separately as well as jointly.

Paired Student's t-test was used to assess statistical difference between measured MBF, PN, and temporal SNR from single-gating and double-gating. *P*-Values < 0.05 were considered statistically significant. Results are reported as mean $\pm$ SD across subjects.

RESULTS

There were no significant differences in measured heart rates between single-gating (71 ± 12 bpm; range, 46–102 bpm) and double-gating (70 ± 13 bpm; range, 47–102 bpm), ($P = 0.17$). There were also no significant differences in measured HRV between single-gating (3.2 ± 2.2 bpm; range 0.2–6.3) and double-gating (2.7 ± 2.3 bpm; range 0.5–7.8 bpm) ($P = 0.22$).

Figure 2 shows MBF and PN maps from two representative subjects measured with single-gating and double-gating methods. It can be observed that PN is lower with double-gating compared with single-gating in both subjects. Measured MBF from the two methods are similar except for two segments (Figure 2, arrows) in the first subject. This discrepancy may be explained by higher PN in the same two segments in single-gating (Figure 2, arrowheads).

The differences in global MBF were not significantly different from the noise level ($P = 0.45$), but the differences in per-segment MBF were statistically significant from the noise level ($P = 0.004$). In this study, neither single-gating nor double-gating is the ground-truth. Therefore, significant differences in MBF measured from the two methods may be expected, especially in high HRV subjects.

Figure 3 shows global PN measurements for double-gating and single-gating as a function of HRV. Double-gating provided consistent PN across HRV while single-gating PN increased with HRV.

Supporting Table S1, which is available online, compares per-segment MBF, PN, and temporal SNR between single-gating and double-gating in the two subgroups. There were significant reductions in PN in low ($P = 0.04$) and high ($P < 0.001$) HRV groups, and improvements in temporal SNR in low ($P = 0.03$) and high ($P = 0.004$) HRV groups without significant differences in measured MBF.

Figure 4 shows linear regression and Bland-Altman analysis of measured global MBF from single-gating and double-gating methods. Bland-Altman reveals no significant bias and paired student's t-test shows no significant difference ($P > 0.69$).

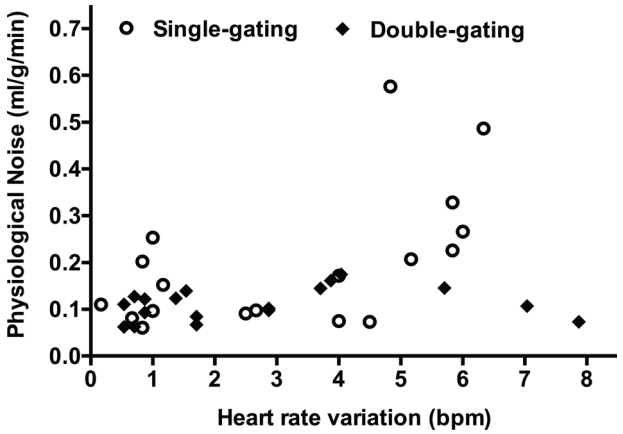

FIG. 3. PN as a function of HRV for single-gating (circle) and double-gating (square). Double-gating is robust to HRV (PN did not depend on HRV). In contrast, single-gating PN increased with HRV.

The mean ± SD of global and per-segment MBF, PN, and temporal SNR from the two methods for all subjects are listed in Table 1. Double-gating demonstrates significant reductions in global and per-segment PN ($P = 0.01$ and $P < 0.001$, respectively) with increased global and per-segment temporal SNR ($P = 0.02$ and $P < 0.001$, respectively) compared with the reference single-gating method. There is no statistically significant difference in measured global and per-segment MBF between the two methods ($P = 0.69$ and $P = 0.95$, respectively).

It is worth noting that residual of fit was used in Poncelet et al (10), as a surrogate for measurement variability. In our study, global double-gating residual of fit and global double-gating PN were 0.10 ± 0.04 and 0.11 ± 0.03 mL/g/min, ($P = 0.28$), respectively. Per-segment double-gating residual of fit and per-segment double-gating PN were 0.18 ± 0.10 and 0.21 ± 0.12 mL/g/min, ($P < 0.0001$), respectively.

DISCUSSION

This study demonstrates that double-gated myocardial ASL is robust to HRV compared with current single-gated techniques, and provides significantly improved temporal SNR. The current double-gating implementation overcomes two main limitations of its predecessor: prohibitively long scan times, and high measurement variability. This study showed that double-gated myocardial ASL is feasible in 3 min of scan time, with a lower noise level in MBF measurements in comparison to the more widely used single-gating method (16–18).

Single-gating has been widely adopted in recent years due to the ease of implementation and quantification. This study demonstrated the feasibility of double-gating with superior temporal SNR efficiency compared with single-gating without significant difference in measured MBF. Superior temporal SNR directly translates to superior sensitivity to measured MBF that, in turn, may be used to reduce total scan time, increase spatial resolution, and/or increase spatial coverage. This finding is expected because in both control and labeled images, labeling and imaging are triggered to occur in the same cardiac phase. Consequently, double-gating is less sensitive to HRV and cardiac motion (both in-plane and though-plane) compared with single-gating.

Over all subjects, double-gating provided significant reduction in PN with increased temporal SNR. The significant PN reduction and temporal SNR increase were found in both low and high HRV groups, but were more pronounced in the high HRV group (when HRV ≥ 4 beats per minute). PN reduction may be clinically important when myocardial perfusion reserve ($MPR = MBF_{stress}/MBF_{rest}$) is used for evaluating severity of CAD based on a cutoff MPR value. A reduction of PN of 0.1 mL/g/min would alter MPR by ~10% (with an assumption that normal $MBF_{rest} = 1.0$ mL/g/min).

The cutoff HRV of 4 bpm was chosen based on the PN data splay for single-gating ASL at HRV > 4 bpm, as seen in Figure 1. All subjects were equally divided into two subgroups (high HRV versus low HRV) to perform comparisons between double-gating and single-gating in terms of temporal SNR. It would be better to relate to different cardiac phases when grouping these subjects with respect to HRV. However, this would require the knowledge of the quiescent diastolic duration, which is patient specific and heart rate dependent. The mid-diastolic quiescence has been shown to vary within the same subject even after normalization to heart rate duration (34).

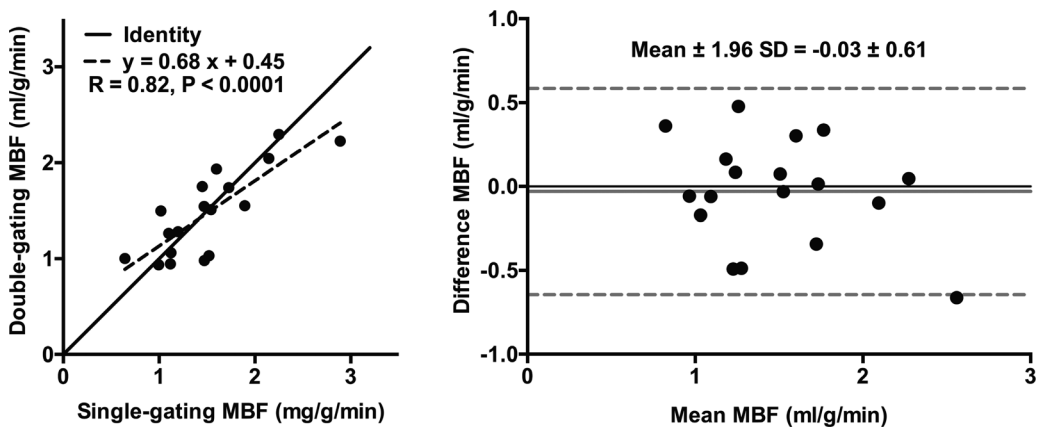

FIG. 4. Comparisons of global MBF measured from single-gating and double-gating using linear regression (left) and Bland-Altman analysis (right). Bland-Altman plot reveals no significant bias between measured MBF from the two methods ($P = 0.69$).

Table 1
Comparison of Global and Per-Segment Myocardial ASL Data Quality with Single-Gating and Double-Gating from All Subjects[a].

	Global (n = 18)			Per-segment (n = 18, 108 segments)		
	MBF (mL/g/min)	PN (mL/g/min)	Temporal SNR (MBF/PN)	MBF (mL/g/min)	PN (mL/g/min)	Temporal SNR (MBF/PN)
Single-gating	1.51 ± 0.54	0.20 ± 0.15	11 ± 8	1.54 ± 0.80	0.33 ± 0.23	7 ± 4
Double-gating	1.48 ± 0.45	0.11 ± 0.03	16 ± 8	1.54 ± 0.67	0.21 ± 0.12	11 ± 12
P-Value	NS (0.69)	0.01	0.02	NS (0.95)	<0.001	<0.001

[a]Double-gating provides significant PN reduction and temporal SNR increase without significant difference in measured MBF compared to single-gating. MBF, PN, and temporal SNR are shown in Mean ± SD format. NS = not significant.

In our study, neither single-gating nor double-gating is the ground-truth. Therefore, differences in MBF measured from the two methods may be expected, especially in subjects with high HRV. Despite the fact that we are comparing two different ASL methods, the differences in MBF measured from the two methods in our study are within the range reported in the myocardial ASL literature for test–retest variability from the same method. Our within subject coefficient of variation was 12.1%, which is smaller than that (21.8%) reported in Wang et al (15). The Bland-Altman plot shows a 95% confidence interval of (-0.58, 0.64 mL/g/min), which is similar to the interobserver variability (−0.77, 0.47 mL/g/min) reported in Northrup et al (14). Our confidence interval is also in the range of inter- and intraobserver variability reported in Capron et al (19).

HRV may arise from numerous sources including sinus arrhythmias, other arrhythmias, and changes in heart rate due to anxiety, patient motion, deep breathing, or arousals from sleepiness during the MRI exam. HRV is closely correlated with image artifacts in computed tomography coronary angiography (25,26), with a reported HRV range of 0–18.1 bpm in one study (26) and 10.9 ± 4 bpm in another (25). HRV was also reported in pharmacologic stress tests to be 18 ± 18 bpm during rest and 16 ± 22 bpm during adenosine infusion (28). Therefore, double-gating is expected to be useful in the clinical setting.

In double-gating, T_1 curve fitting was used as part of MBF quantification. In this process, a precise inversion time was crucial for accurate T_1 curve fitting as acknowledged by Zhang et al (13). We implemented the "adaptive recovery time" method (30) where, after an inversion pulse, a series of 2-ms wait-pulses are played until the next detected R-wave to allow precise and consistent measurements of inversion.

Our double-gated module is identical to that in Poncelet et al (10), but there are several differences in our implementation including field strength and imaging sequence. Our experiments were performed on a 3T scanner compared with 1.5T in Poncelet's work. The higher field strength is beneficial for cardiac ASL because of higher intrinsic SNR and longer T_1 relaxation times, both of which improve the strength of the ASL signal. Another difference is that we used snapshot balanced SSFP for image acquisition compared with single-shot echo planar imaging (EPI) in the prior study. Single-shot EPI suffers from image distortion as well as signal loss due to magnetic field inhomogeneity. Balanced SSFP, on the other hand, is free of distortion and provides superior SNR efficiency. This sequence was not widely used at the time of Poncelet's work, because it relies on fast gradients and shimming. Both higher SNR and longer T_1 relaxation time directly translates to the improved temporal stability and intrascan variability of our method.

The study has several limitations. Only a small number of healthy subjects and heart transplant recipients were recruited. Systematic evaluations of double-gating on larger cohorts are warranted for future study. There was no ground-truth for MBF in this study. First-pass MRI and SPECT may be used for comparison but were not available in this cohort. Double-gating may also be validated in an animal model where first-pass perfusion, microspheres, or positron emission tomography may be used as the reference standard. Only a single, midventricular short axis slice was acquired in this study. In this study, inversion was used for labeling pulse; however, the use of saturation labeling may allow for complete data acquisition within two breath-holds instead of seven breath-holds, potentially allowing for acquisition of three sequential slices in the same scan time as single-slice with inversion labeling. The feasibility and repeatability of saturation double-gated myocardial ASL remains to be explored in future work.

CONCLUSIONS

This study demonstrates that double-gated myocardial ASL is robust to HRV in comparison to single-gated myocardial ASL. This, in turn, leads to superior temporal SNR efficiency of double-gating compared with single-gating. This is expected to be valuable for stress testing under physiologic or pharmacologic stress.

ACKNOWLEDGMENT

H.P.D. was partially supported by a Merit Fellowship from USC Danna and David Dornsife College of Letters, Arts, and Sciences.

REFERENCES

1. Cerqueira MD, Allman KC, Ficaro EP, Hansen CL, Nichols KJ, Thompson RC, Van Decker WA, Yakovlevitch M. Recommendations for reducing radiation exposure in myocardial perfusion imaging. J Nucl Cardiol 2010;17:709–718.
2. Fazel R, Dilsizian V, Einstein AJ, Ficaro EP, Henzlova M, Shaw LJ. Strategies for defining an optimal risk-benefit ratio for stress myocardial perfusion SPECT. J Nucl Cardiol 2011;18:385–392.
3. Greenwood JP, Maredia N, Younger JF, et al. Cardiovascular magnetic resonance and single-photon emission computed tomography for

diagnosis of coronary heart disease (CE-MARC): a prospective trial. Lancet 2012;379:453–460.
4. Khawaja AZ, Cassidy DB, Al Shakarchi J, McGrogan DG, Inston NG, Jones RG. Revisiting the risks of MRI with Gadolinium based contrast agents—review of literature and guidelines. Insights Imaging 2015;6: 553–558.
5. Perazella MA. Nephrogenic systemic fibrosis, kidney disease, and gadolinium: is there a link? Clin J Am Soc Nephrol 2007;2:200–202.
6. Detre JA, Leigh JS, Williams DS, Koretsky AP. Perfusion imaging. Magn Reson Med 1992;23:37–45.
7. Alsop DC, Detre JA, Golay X, et al. Recommended implementation of arterial spin-labeled perfusion MRI for clinical applications: a consensus of the ISMRM perfusion study group and the european consortium for ASL in dementia. Magn Reson Med 2014;116:102–116.
8. Telischak NA, Detre JA, Zaharchuk G. Arterial spin labeling MRI: clinical applications in the brain. J Magn Reson Imaging 2015;41: 1165–1180.
9. Epstein FH, Meyer CH. Myocardial perfusion using arterial spin labeling CMR: promise and challenges. JACC Cardiovasc Imaging 2011;4:1262–1264.
10. Poncelet BP, Koelling TM, Schmidt CJ, Kwong KK, Reese TG, Ledden P, Kantor HL, Brady TJ, Weisskoff RM. Measurement of human myocardial perfusion by double-gated flow alternating inversion recovery EPI. Magn Reson Med 1999;519:510–519.
11. Wacker CM, Fidler F, Dueren C, Hirn S, Jakob PM, Ertl G, Haase A, Bauer WR. Quantitative assessment of myocardial perfusion with a spin-labeling technique: preliminary results in patients with coronary artery disease. J Magn Reson Imaging 2003;18:555–560.
12. Fidler F, Wacker C, Dueren C, Weigel M, Jakob P, Bauer W, Haase A. Myocardial perfusion measurements by spin labeling under different vasodynamic states. J Cardiovasc Magn Reson 2004;6:509–516.
13. Zhang H, Shea SM, Park V, Li D, Woodard PK, Gropler RJ, Zheng J. Accurate myocardial T1 measurements: toward quantification of myocardial blood flow with arterial spin labeling. Magn Reson Med 2005;53:1135–1142.
14. Northrup BE, McCommis KS, Zhang H, Ray S, Woodard PK, Gropler RJ, Zheng J. Resting myocardial perfusion quantification with CMR arterial spin labeling at 1.5 T and 3.0 T. J Cardiovasc Magn Reson 2008;10:53.
15. Wang DJJ, Bi X, Avants BB, Meng T, Zuehlsdorff S, Detre JA. Estimation of perfusion and arterial transit time in myocardium using free-breathing myocardial arterial spin labeling with navigator-echo. Magn Reson Med 2010;64:1289–1295.
16. Zun Z, Wong EC, Nayak KS. Assessment of myocardial blood flow (MBF) in humans using arterial spin labeling (ASL): feasibility and noise analysis. Magn Reson Med 2009;62:975–983.
17. Zun Z, Varadarajan P, Pai RG, Wong EC, Nayak KS. Arterial spin labeled CMR detects clinically relevant increase in myocardial blood flow with vasodilation. JACC Cardiovasc Imaging 2011;4:1253–1261.
18. Do HP, Jao TR, Nayak KS. Myocardial arterial spin labeling perfusion imaging with improved sensitivity. J Cardiovasc Magn Reson 2014; 16:15.
19. Capron T, Troalen T, Robert B, Jacquier A, Bernard M, Kober F. Myocardial perfusion assessment in humans using steady-pulsed arterial spin labeling. Magn Reson Med 2015;74:990–998.
20. Kim SG. Quantification of relative cerebral blood-flow change by flow- sensitive alternating inversion-recovery (fair) technique - application to functional mapping. Magn Reson Med 1995;34:293–301.
21. Kwong KK, Chesler DA, Weisskoff RM, Donahue KM, Davis TL, Ostergaard L, Campbell TA, Rosen BR. MR perfusion studies with T1-weighted echo planar imaging. Magn Reson Med 1995;34:878–887.
22. Buxton RB, Frank LR, Wong EC, Siewert B, Warach S, Edelman RR. A general kinetic model for quantitative perfusion imaging with arterial spin labeling. Magn Reson Med 1998;40:383–396.
23. Clynes M. Computer analysis of reflex control and organization: respiratory sinus arrhythmia. Science 1960;131:300–302.
24. Raper AJ, Richardson DW, Kontos HA, Patterson JL. Circulatory responses to breath holding in man. J Appl Physiol 1967;22:201–206.
25. Leschka S, Wildermuth S, Boehm T, et al. Noninvasive coronary angiography with 64-section CT: effect of average heart rate and heart rate variability on image quality. Radiology 2006;241:378–385.
26. Sun G, Li M, Jiang X-S, Li L, Peng Z-H, Li G-Y, Xu L. 320-detector row CT coronary angiography: effects of heart rate and heart rate variability on image quality, diagnostic accuracy and radiation exposure. Br J Radiol 2012;85:e388–e394.
27. Jouven X, Schwartz PJ, Escolano S, Straczek C, Tafflet M, Desnos M, Empana JP, Ducimetire P. Excessive heart rate increase during mild mental stress in preparation for exercise predicts sudden death in the general population. Eur Heart J 2009;30:1703–1710.
28. Okada DR, Ghoshhajra BB, Blankstein R, et al. Direct comparison of rest and adenosine stress myocardial perfusion CT with rest and stress SPECT. J Nucl Cardiol 2009;17:27–37.
29. Vembar M, Garcia MJ, Heuscher DJ, Haberl R, Matthews D, Bohme GE, Greenberg NL. A dynamic approach to identifying desired physiological phases for cardiac imaging using multislice spiral CT. Med Phys 2003;30:1683–1693.
30. Slavin GS, Stainsby JA. True T1 mapping with SMART 1 Map (saturation method using adaptive recovery times for cardiac T 1 mapping): a comparison with MOLLI. J Cardiovasc Magn Reson 2013;15: P3.
31. Griswold MA, Jakob PM, Heidemann RM, Nittka M, Jellus V, Wang J, Kiefer B, Haase A. Generalized autocalibrating partially parallel acquisitions (GRAPPA). Magn Reson Med 2002;47:1202–1210.
32. Le Roux P. Simplified model and stabilization of SSFP sequences. J Magn Reson 2003;163:23–37.
33. Cerqueira MD, Weissman NJ, Dilsizian V, Jacobs AK, Kaul S, Laskey WK, Pennell DJ, Rumberger JA, Ryan TJ, Verani MS. Standardized myocardial segmentation and nomenclature for tomographic imaging of the heart. J Cardiovasc Magn Reson 2002;4:203–210.
34. Ravichandran L, Wick CA, Tridandapani S. Detection of quiescent phases in echocardiography data using non-linear filtering and boundary detection. Conf Proc IEEE Eng Med Biol Soc 2012;2012: 1562–1565.

SUPPORTING INFORMATION

Additional Supporting Information may be found in the online version of this article.

Table S1. Comparison of Per-Segment MBF, PN, and Temporal SNR between Double-Gating and Single-Gating with Respect to HRV. Double-gating shows significant reduction in PN and significant increase in temporal SNR without significant difference in measured MBF compared to single-gating in both subgroups, but it is more pronounced in the high HRV group. MBF, PN, and temporal SNR are shown in mean ± SD format. NS = not significant.